Stony Brook University

Fabrication and Applications of Electrospun Core-sheath Fibers

A Thesis Presented

by

Shifeng Han

to

the Graduate School

in Partial Fulfillment of the

Requirements

for the Degree of

Master of Science

in

Chemistry

Stony Brook University

May 2010

Stony Brook University

The Graduate School

Shifeng Han

We, the thesis committee for the above candidate for the

Master of Science degree, hereby recommend

acceptance of this thesis.

Benjamin Chu – Thesis Advisor
Professor, Chemistry Department

David Hanson – Chairperson of Defense
Professor, Chemistry Department

Stanislaus Wong – Third Member
Professor, Chemistry Department

This thesis is accepted by the Graduate School

Lawrence Martin
Dean of the Graduate School

Abstract of the Thesis

Fabrication and Applications of Electrospun Core-sheath Fibers

by

Shifeng Han

Master of Science

in

Chemistry

Stony Brook University

2010

Interests in electrospinning have recently been expanded further due to the ability of electrospinning to produce nanofibers with core-sheath or hollow structures. Such fibers have been widely studied as a promising candidate for many applications, such as biomedical and electrical devices. This thesis has been composed of two parts on the coaxial electrospinning technology: (1) an overview of the coaxial electrospinning, including its essential features, the material and process parameters that can impact fiber formation, and the potential applications of core-sheath fibers; (2) a research study on electrospun poly(ethylene glycol)-poly(ε-caprolactone) (PEG-PCL) core-sheath structured fibers. The research project included the fabrication of core-sheath structured fibers, the extraction of PEG from the fibers, and the characterization of core-sheath fibers.

Table of Contents

List of Equations

List of Figures

List of Tables

Acknowledgements:

I would like to thank my advisors, Professor Benjamin Chu and Professor Benjamin S. Hsiao for giving me such detailed guidance, very useful advices and lots of good ideas on revising my thesis. This thesis would not have been possible without their supports.

I have also benefited from discussions with many other professors in the Chemistry Department. I particularly would like to thank my committee members, Professor David Hanson and Professor Stanislaus Wong, for their valuable suggestions and encouragement. Thanks also to Dr. James Marecek for helping me with the ^{1}H NMR measurement in this project.

Lastly, I am grateful to Dr. Hongyang Ma, Dr. Fan Wan, Dr. Dufei Fang and all the other Chu/Hsiao group members for their kindly help in my research and daily life.

1. Introduction

In the early 1900s, Cooley and Morton invented electrospinning, based on Gray's observation of water behavior under the influence of electrostatics [1]. For most of the last century, this technology did not receive much attention, partly because of the intrinsic complexity associated with such a process. In the 1990s, researchers in nanoscience and nanotechnology gradually realized the importance of this technology, resulting in a flourishing of activities [1]. One of the attractive features of electrospinning is the ability to fabricate ultra-fine polymeric fibers from submicron diameters down to nanometer diameters. There are many potential advantages associated with non-woven nanofibrous mats, such as large surface areas per unit mass and very small effective 'pore' sizes. The single-spinneret electrospinning setup is composed of a syringe pump, a high voltage source, a spinneret and a collector, as shown schematically in Fig. 1.

During the electrospinning process, when a polymer solution is flowing out of the spinneret under an applied electric field, a cone-shaped droplet is formed, commonly called the "Taylor cone" [2-4]. When the applied voltage is strong enough to overcome the surface tension of the polymer solution, a fine jet stream of the polymer solution is ejected from the surface of the droplet and is being drawn toward the collector. As this jet stream travels, the solvent is being evaporated, resulting in the formation of a non-woven fibrous scaffold in the collector. The fiber diameter and the morphology are mainly affected by both processing and material parameters [5-10, 26], such as solution properties (e.g., concentration, viscosity and conductivity), applied voltage, solution flow-rate and distance between the spinneret tip and the collector. These parameters for generating nanofibers using the electrospinning process have been studied and summarized in a review [11]. Synthetic and natural polymers have

been electrospun into fibers, such as polyglycolide (PGA) [12], polylactide (PLA) [13] and Poly(ε-caprolactone) (PCL) [14]; collagen [15], gelatin [16] and silk fibroin [17]. These electrospun fibrous scaffolds offer a broad range of applications, including tissue engineering scaffolds [18-22], drug-delivery system [23-25], filtration and gas storage [26, 27], and sensors and electrodes for use in electronics [28].

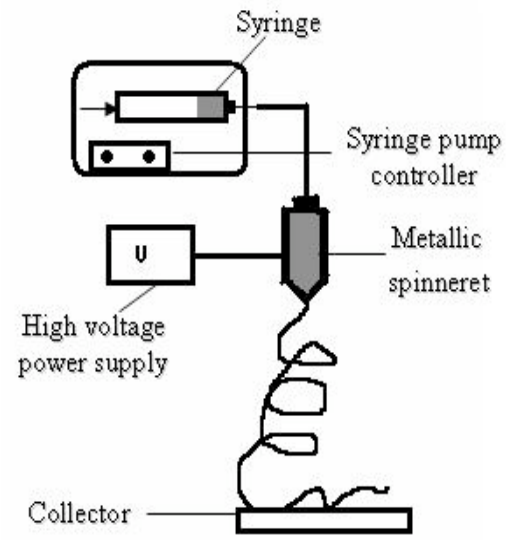

Figure 1 Single-spinneret electrospinning setup

Very recently, the demand of special polymeric fibers, such as core-sheath fibers and hollow fibers, has engaged the interests of polymer scientists and engineers to develop a new device for the preparation of core-sheath structured fibers. In this process, a special spinneret composed of two coaxial capillaries was developed for electrospinning by using two polymer solutions into core-sheath fibers [29-56]. With proper processing conditions, the core component can be encapsulated inside the nanofiber shell. Compared with other methods widely used for encapsulation, this coaxial technique has the advantages of having a high loading efficiency, easier processing, and relatively stabilized release characteristics. Such

core-sheath fibers offer a wide range of potential uses [29-31, 37-55]: to isolate an unstable component in the core so as to avoid its decomposition under an aggressive environment, to deliver a substance to a particular receptor with the drug being encapsulated in the core, to improve the mechanical properties of both components, and to serve as a scaffold for tissue engineering in which a less biocompatible polymer is surrounded by a more biocompatible material.

Using the core-shell approach, a non-spinnable polymer or powder can be coaxially electrospun to form a core within the sheath of other spinnable polymers. In addition, hollow structured nanotubes can be generated after the removal of the core material [46]. Another advantage of such core-sheath fibers is that the sheath layer cannot only provide the protection of encapsulated bioactive agents, but also control the drug release rate. Electrospun drug-loaded polymer fibers often show a significant burst release because the drug particles tend to be located on the surface of fibers [57]. By contrast, coaxial electrospinning can homogenously encapsulate bioactive agents into the polymer sheath in order to achieve a more stable and controlled release profile [34, 52, 55]. Numerous studies have been published on the coaxial electrospinning process for preparing core-sheath structured fibers for various applications.

In this thesis, an overview of the coaxial electrospinning technology, including its essential features, some materials and process parameters that impact fiber formation, and potential applications of core-sheath nanofibers is presented. The second part of this thesis is devoted to the experimental work that has been carried out at Stony Brook University, including the fabrication of core-sheath structured fibers, the extraction of PEG from the fibers, and the characterization of core-sheath structured fibers.

2. Coaxial Electrospinning

2.1. General setup

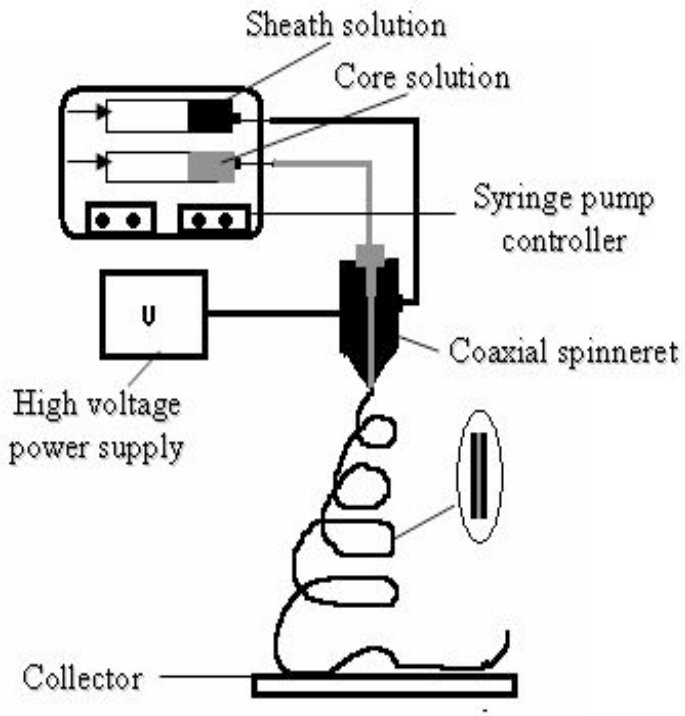

Figure 2 Coaxial electrospinning setup.

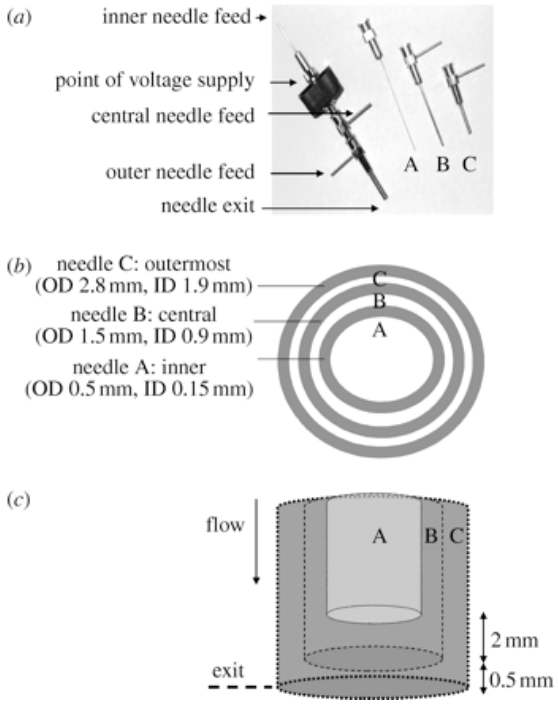

Figure 3 Details of the tri-needle coaxial device. Reprinted from reference [35].

Like regular electrospinning, coaxial processing also relies on the electrical force on polymer solution to overcome surface tension and to stretch the jet stream of concentrated polymer solution with concurrent solvent evaporation, resulting in the formation of extremely fine fibers at a collector. The basic setup of coaxial electrospinning is shown schematically in Fig. 2.

The special spinneret is a key component of the coaxial device, which is modified by concentrically inserting a smaller diameter (core) capillary into a larger diameter (sheath) capillary to make up the coaxial configuration. Two polymer solutions are fed through the two concentrically arranged capillaries under a proper electrostatic field in order to achieve continuous core-sheath structured fibers. In general, the flow-rates of the two solutions are controlled by separate programmable pumps [32, 37-55]. However, in some studies, the

sheath solution was open to the atmosphere and was allowed to flow due to gravity [31, 33, 34].

The coaxial setup requires a carefully designed spinneret, especially with respect to outer and inner capillary diameters. Table 1 lists some selective outer/inner-capillary diameters of coaxial spinneret from various studies [21, 36, 42, 46, 51, 53]. However, no systematic study has been performed on the capillary diameters. Thus, more characterizations are needed in order to better understand the effects of outer and inner capillary diameters on fiber morphology and size. Recently, a different spinneret has been reported by Ahmad et al. [35], which used a tri-needle coaxial device as shown in Fig. 3. This new design consists of three separate needles with different diameters of outermost, central and inner tubes in the range of 1.9 mm, 0.9 mm and 0.15 mm, respectively. The authors stated that electrospun three-layer fibers have the potential for multiple loading of drugs, prodrugs or other agents that could be released at different times and different amounts. To date, this tri-needle coaxial device has not been widely studied by other researchers.

	Needle-Diameter	
Reference	**Outer**	**Inner**
Li et al. [46]	200 μm	75 or 100 μm
Huang et al. [21]	1.6 mm	0.8 mm
Zhang et al. [51]	2.5 mm	1.1 mm
Zhao et al. [53]	0.9 mm	0.57 mm
Bazilevsky et al. [42]	0.82 mm	0.51 mm
Li et al. [36]	1.6 mm	0.8 mm

Table 1 List of outer/inner-needle diameters for a coaxial spinneret.

The process of coaxial electrospinning is theoretically similar to that of the regular electrospinning [36-38]. When two charged immiscible polymer solutions are concentrically

flowing out of the coaxial spinneret under an applied high voltage, a conical shape droplet is formed. A tiny jet is ejected once the charge accumulation on the droplet reaches a certain value due to an increase in the applied voltage. As long as the Taylor cone is stable, the core solution can be uniformly encapsulated into the sheath. On the way to a collector, the solvent in the core and that in the sheath evaporate, and the core-sheath fibers are formed (Fig. 4).

Although the process of coaxial electrospinning is similar to that of the general electrospinning, the materials and processing parameters that control the process of fiber formation become more complicated since both the sheath and the core solution conditions should be taken into account at the same time. A brief review of the materials and processing parameters are given below.

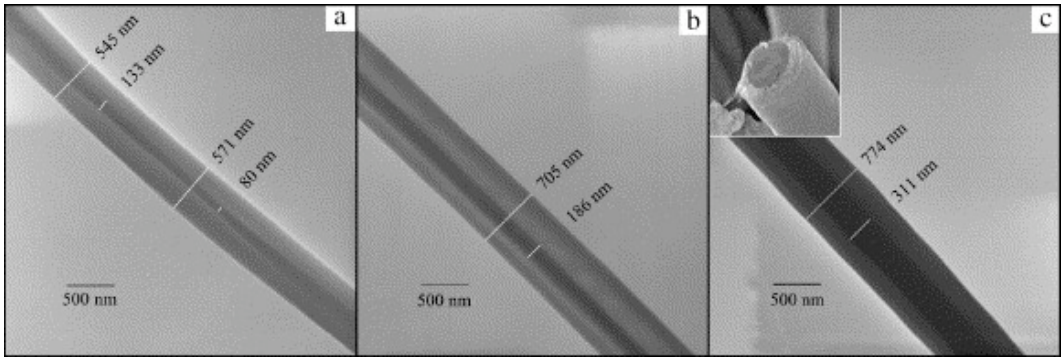

Figure 4. Core-sheath structured fibers composed of PCL as sheath and BSA/PEG as core prepared by coaxial electrospinning. The flow-rate of the inner solution was (a) 0.6, (b) 1 and (c) 2 ml/h, respectively. Reprinted from Reference [34]

2.2. Material and process parameters

During the process of coaxial electrospinning, materials and processing parameters play a very important role in the formation of core-sheath structured fibers. Table 2 shows several significant parameters. The effects of the materials properties are very difficult to isolate because varying one parameter can generally affect other solution parameters. For

example, changing the solution concentration can also change the viscosity and conductivity. By contrast, the process parameters are more controllable. In this section, we investigate the effect of each parameter on the fiber morphologies and diameters.

Material Parameters	Process Parameters
▪ Solution Concentration*	▪ Applied Voltage*
▪ Solution Viscosity*	▪ Solution Flow-rate*
▪ Solvent/Solution Miscibility*	▪ Spinneret tip-to-collector distance
▪ Solution Conductivity*	▪ Collector rotating speed
▪ Solvent Vapor Pressure	

Table 2 List of material and process parameters for coaxial process. The parameters with * will be explained in more detail.

2.2.1. Material parameters

Solution concentration and viscosity: Solution concentration and viscosity were found to be among the important parameters for the formation of fiber morphology during the electrospinning process. The relationship between the polymer viscosity and concentration has been investigated in several studies [29, 39, 40, 41]. In general, an increase in the solution concentration increases its viscosity.

During the coaxial electrospinning, the sheath solution guides the flow of the core material in the jet stream. Moghe et al. [29] demonstrated that the sheath solution should be sufficiently viscous in order to overcome the interfacial tension between the two solutions, resulting in a stable Taylor cone. In contrast, the core solution could be a fluid that does not satisfy the general requirements for electrospinning. As suggested by Bazilevsky et al. [42], a non-polymeric liquid or even a powder could be used as the inner core.

The diameters of both core and sheath produced by coaxial electrospinning were found to increase with increasing either core or sheath solution concentration [34, 44, 45, 55], which was due to an increase in the amount of polymer in the jet stream. For example, Zhang et al. [45] reported that by increasing the core concentration (core: gelatin; sheath: poly(caprolactone) (PCL)) from 7.5 to 12.5 w/v%, an increase in the core size and overall fiber diameter from ~100 to ~200 nm and ~250 to ~350 nm, respectively, was observed. In a study by He et al. [55], they reported that the average fiber diameter corresponding to the sheath concentration of 5, 8, and 10 wt% were 360, 1095, and 1312 nm, respectively (core: tetracycline hydrochloride (TCH); sheath: poly-L-Lactic acid (PLLA)). This result indicated that an increase in the sheath concentration also increased the overall fiber diameter.

Wei et al. [43] studied the effects of viscosity ratio of two solutions. They reported that the viscosity ratios between the core and the sheath were not important in the formation of core-sheath structures. However, they found that the viscosity values played a significant role in determining which polymer was the core material and which polymer was the sheath since the sheath solution always required a higher viscosity value in order to efficiently encapsulate the core solution.

Solvent/solution miscibility: The interaction between core and sheath solution is crucial for coaxial electrospinning. Two approaches regarding solvent/solution miscibility have been reported by Moghe et al. [29]: (1) When the two solutions were ejected from the spinneret, the solvents used in either core or sheath should not precipitate the polymer from the other solution; (2) The interfacial tension between the two fluids should be kept as low as possible for stabilizing the Taylor cone.

Two opposite opinions on the miscibility of core and sheath solution were reported by different researchers. As suggested by Wei et al. [43] and Li et al. [46, 47], two miscible solutions should not be used for the coaxial process since they would dissolve each other when they meet at the tip of the spinneret, resulting in a diffused interface of core and sheath layers. The use of two immiscible solutions, such as the fabrication for a hydrophobic sheath and a hydrophilic core, was the key to produce continuous fibers with a core-sheath structure. In the work by Li et al. [47], they used two immiscible solutions, poly(vinyl pyrrolidone) (PVP)/$Ti(OiPr)_4$ as the sheath and heavy mineral oil as the core, and obtained ultrafine core-sheath structured fibers. However, they repeated the experiment by using miscible PVP solution instead of the mineral oil as the core, and no core-sheath structured fibers were formed. Sun et al. [44] had successfully electrospun two immiscible solutions (core: hydrophilic PVP; sheath: hydrophobic poly(D,L-lactide) (PLA)) into uniform core-sheath fibers. These results were in agreement with their hypothesis. Additionally, Li et al. [46, 47] emphasized that two miscible solvents could not be used in two immiscible polymers since the evaporation and diffusion of the solvents would drive the two polymers to mix together. In an effort to verify this hypothesis, they used two immiscible polymers (core: polystryrene; sheath: PVP) dissolved in two miscible solvents (core: N, N-dimethylformamide (DMF)/tetrahydrofuran (THF); sheath: ethanol) for another study. The electrospun fibers did not show core-sheath structure.

On the other hand, Han et al. [48] reported that two miscible solutions could still produce core-sheath structured fibers since the inter-diffusion time between the two solutions was much longer than the travel time of the liquid jet stream from the needle to the collector. In other words, the short time duration of the process prevented the two fluids from mixing

significantly. Yu et al. [49] carried out a series of experiments to demonstrate that with proper electrospinning conditions, two miscible solutions, such as polyacrylonitrile/poly(acrylonitrile-co-styrene) (PAN/PAN-co-PS), poly(aniline sulfonic acid)/poly(vinyl alcohol) (PAni/PVA), and Bombyx mori silk/poly(ethylene oxide) (Silk/PEO), could form ultrafine core-sheath fibers. Moreover, the authors emphasized that using a common solvent and/or two miscible solutions helped to reduce the interfacial tension between the two solutions, resulting in the production of even smaller diameter fibers. Huang et al. [21] used the same solvent, ethanol, in both the core (resveratrol (RT)) and the sheath (PCL) solution, and achieved core-sheath structured fibers. Zhang et al. [31] also reported that core-sheath fibers could be prepared from PCL and gelatin dissolved in the same solvent, tetrafluoroethylene.

Most of the researchers [21, 31, 44, 49, 55] have agreed that with proper process condition, either miscible or immiscible solutions/solvents can be successfully electrospun into core-sheath structured fibers.

Solution conductivity: Few studies have systematically investigated the effects of solution conductivity and charge density on the electropun fiber morphology. In general, high conductivity solutions have high surface charge density, which produce smaller diameter fibers with a faster rate due to an increase in the elongational force on the jet under a given electrical field.

A report by Yu et al. [49] showed that a third of the electrospun PAni-PVA fibers did not display a continuous thread of the PAni in the core. Based on this result, the authors speculated that the PAni solution (core) had higher charge density than the PVA solution

(sheath), which was being pulled by the applied voltage at a faster rate than the feed line could supply, causing a discontinuous core material in the fiber. By contrast, higher sheath conductivity usually would not interrupt the process of core-sheath fiber formation [46]. These results indicate that non-conductive or less conductive liquids as the core can be successfully encapsulated into a higher conducting sheath.

The basic requirements of materials selection were summarized. The electrospinnable sheath solution should have relatively high viscosity and conductivity and there should be low interfacial tension between the sheath and the core solutions.

2.2.2. Process parameters

Applied voltage: The impact of applied voltage on fiber morphology has not been studies widely in the coaxial electrospinning process. In most studies, the authors only provided one critical applied voltage for the generation of a stabilized Taylor cone and jet. Generally, both core and sheath diameters of fibers were decreased with increasing applied voltage. Fig. 5 demonstrates the voltage dependence of the core-sheath fiber formation. At low voltage (subcritical voltage), a big drop forms at the tip of the needle, leading to an increase in beaded fibers. With increasing voltage (critical voltage), the volume of the drop was reduced, resulting in a stable compound Taylor cone. As the voltage was increased further (supercritical voltage), the strength of electrical field could exceed that required for the given material and the processing conditions. Then, the Taylor cone would tend to recede, resulting in forming separate jets from the sheath and core solutions.

In a study by Li et al. [46], they reported that both the core and sheath diameters of the fibers decreased with increasing the strength of applied voltage. For example, an increase

in the applied voltage from 12 to 16 kV reduced the average inner diameter of core-sheath fibers (core: heavy mineral oil; sheath: PVP/$Ti(OiPr)_4$) from 200 to 130 nm, but the wall thickness was kept the same. Huang et al. [21] stated that the applied voltage used in coaxial process generally was higher than that of single-spinneret electrospinning. For example, the generation of pure PCL solution into fibers through the single-fluid electrospinning only required a voltage of 7-8 kV, but the introduction of the pure drug (GS) as the core material significantly increased the magnitude of the applied voltage to 11-13 kV.

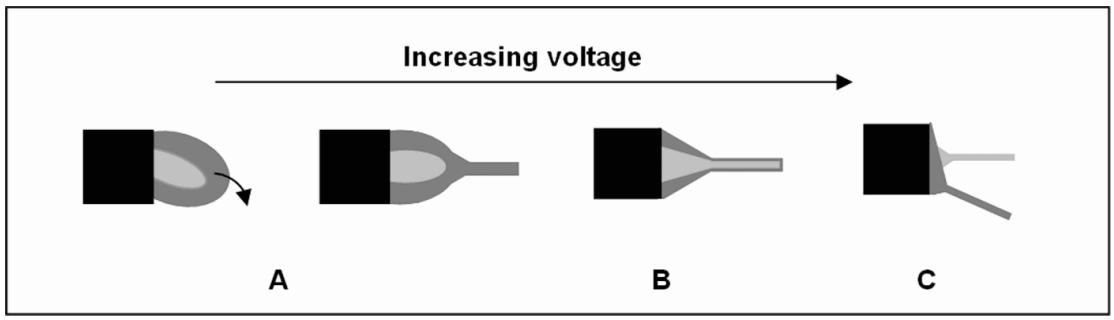

Figure 5 Schematics of voltage dependence on core-sheath fiber formation in coaxial electropsinning (A: Subcritical voltage; B: Critical voltage; C: Supercritical voltage). Reprinted from Reference [29].

Solution flow-rate: One of the most studied parameters among the processing variables is the effect of flow-rates and/or flow-rate ratio. The core diameter and the wall thickness of core-sheath fibers could be conveniently controlled by adjusting the flow-rates of the core solution. For example, in a coaxial process of heavy mineral oil (core) and PVP/$Ti(OiPr)_4$ (sheath), decreasing the flow-rate of the core solution from 0.3 to 0.1 mL/h increased the wall thickness from 20 to 50 nm [50]. By contrast, increasing the flow-rate of the core solution led to the formation of thinner wall.

In addition, both core and sheath solutions should be delivered at appropriate flow-rates to keep the core-sheath jet continuous [51]. If the core flow-rate was too low, the

amount of solution delivered would be insufficient to facilitate a continuous incorporation of the core into the sheath. If the core flow-rate was too high, the core fluid jet would break into droplets. A study by Jiang et al. [52] was in agreement with this hypothesis. They demonstrated that the continuous core-sheath fibers could be generated only if the flow-rate of the core solution (bovine serum albumin (BSA)-containing dextran) was in a stable range of above 0.1 mL/h and below 0.8 mL/h and the flow-rate of the outer solution (PCL) was 1 mL/h, otherwise no smooth core-sheath fibers were formed. Zhao et al. [52] stated that when the flow-rate ratio of core and sheath solutions was not in a stable range, the excess solution would drop out and form the fibers with very heterogeneous size distribution and structure. In most of the studies [43, 44, 46, 48-56], the authors provided the flow-rate ratio of core and sheath solutions for the coaxial electrospinning. For example, Liao et al. [56] showed that in a system of BSA (core) and PCL (sheath), 100% loading efficiency was achieved with a 3:1 sheath/core solution feeding ratio (10 w/v% PCL in 6/4 (v/v) dichloromethane/ethanol solvent; BSA in water). In addition, the core flow-rate has to be lower than that of the sheath to ensure enough sheath materials for encapsulating the fast moving core material uniformly.

3. Properties and applications of core-sheath nanofibers

3.1. Core-sheath nanofibers for controlled-release system

One of the major applications of core-sheath nanofibers is for controlled-release systems [34, 36, 51-56]. Such fibrous membranes are helpful to deliver bioactive agents to a localized area, decrease adverse side effects, increase circulation time in the body, and control release rates [11, 18, 25]. Moreover, the core-sheath fibers can also provide drug release with a rapid, immediate, or delayed manner according to the status of the drugs incorporated in the polymer carrier.

Materials		Solvents		
Core	Sheath	Core	Sheath	Reference
PEG+BSA or lysozyme	PCL	Water	DMF/chloroform 3/7 ratio	Jiang et al. [34]
Dextran+BSA or lysozyme	PCL/PEG	Water	DMF/chloroform 3/7 ratio	Jiang et al. [52]
BSA	PCL/PEG	Water	Dichloromethane/ethanol 6/4 ratio	Liao et al. [56]
Drug-TCH	PLLA	Methanol/chloroform 2/1 ratio	Chloroform/acetone 2/1 ratio	He et al. [55]
Drug-TCH	PLLACL	TFE	TFE	Su et al. [37]
PVP	PLA	DMF/ethanol 1/1 ratio	DMF/acetone 8/2 ratio	Sun et al. [44]
PCL	Gelatin	TFE	TFE	Zhao et al. [52]

Table 3 List of studies using coaxial electrospinning to achieve bioactive agents-encapsulation.

Electrospun drug-loaded polymer nanofibers using the conventional single-fluid electrospinning always show a significant burst release in the initial stage since the (often ionic) drug particles tend to be located on the surface of nanofibers during the electrospinning process [57]. Another drawback is that, during preparation of a mixed

solution of drug(s) and polymer, the long time exposure of bioactive agents to harsh organic solvent would potentially destroy the activity of the encapsulated agents. Ideally, if drugs can be encapsulated homogeneously by polymer, the release profile of drugs would be more stable. Coaxial electrospinning provides an alternative and simple way to encapsulate drugs into fibers more uniformly. As long as the sheath solution is suitable for electrospinning, the core solution can either be or not be suitable for electrospinning. The core-sheath structured fibers by the coaxial electrospinning process reduce the possibility of contact with bioactive agents to organic solvents and could protect the agents from activity loss. The sheath layer plays an important role not only to control the drug release rate, but also to overcome the problem of burst release at an early stage. In electrospun core-sheath nanofibers, the drug release relies mainly on the following pathway: degradation of the sheath layer, diffusion of the drug through the carrier, thickness and/or permeability of the sheath, and pinholes caused by sheath failure (Fig. 6) [34, 52, 55]. Several studies in the drug release are listed in Table 3.

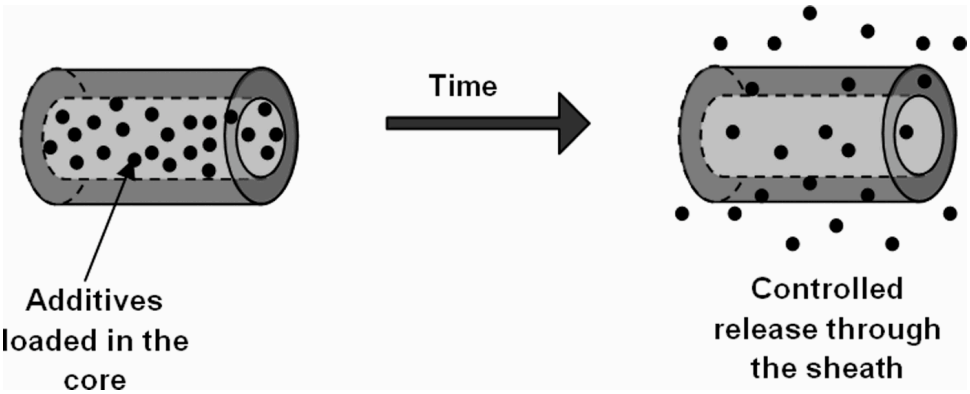

Figure 6 Schematic of micro-encapsulation of additives and controlled release. Reprinted from Reference [29].

In a study by Jiang et al. [34], they reported that the poly(ethylene glycol) (PEG) solution containing BSA or lysozyme as the core and PCL as the sheath could be successfully electrospun into core-sheath structured fibers that could achieve a subsequent

relatively steady release phase with a slight initial burst release. The incorporation of PEG into the core layer could also enhance the stability of fragile bioactive macromolecules and modulate the release characteristics of various agents. The morphology change of the core-sheath fibers after different incubation days is displayed in Fig. 7. Gradual collapse of the nanofibers was observed due to the sustained release of the core content. Along this line, the same authors later showed a more refined study using aqueous dextran solution containing BSA or lysozyme as the core and PCL and PEG as the sheath [52]. The results clearly showed that the release rates were depended on the amount of PEG in the sheath because PEG acted as a pore-forming agent resulting from its water solubility and the phase-separated morphology of the fibers. For example, increasing the amount of PEG in the sheath layer from 5 to 40% resulted in an increase of BSA release from 40-67%. In addition, the authors stated that the protein stability could be enhanced by the presence of dextran. Similarly, Liao et al. [56] have also reported that by incorporating PEG into the sheath of PCL fibers to serve as a porogen, the release rate of the encapsulated protein BSA could be controlled by the molecular weight and concentration of PEG. Increasing the PEG (M_w 8000 g/mol) concentration from 1 to 20 mg/ml in PCL-based sheath fibers enhanced the protein release kinetics from ~65 to 85% on day 40. By contrast, without incorporation of PEG into the PCL phase led to a slowest release rate of BSA, ~50% on day 40. The degree of swelling and pore formation of fiber were mainly controlled by the molecular weight of PEG (M_w 1050, 3400, and 8000 g/mol) that was incorporated into the PCL layer.

He et al. [55] reported that a drug, TCH, has been successfully incorporated into PLLA by coaxial electrospinning. The authors showed that the release-rates of the drug could be easily controlled by adjusting the thickness of the sheath layer that could be changed by

using different concentrations of the sheath solutions. For example, in a 30-day period, the fibers fabricated by 5 wt% PLLA showed ~55% release rate of the drug; by contrast, the fibers fabricated by 10 wt% PPLA only released ~44% TCH. Additionally, PLLA concentrations also affected the tensile strength of fibers. The authors found that the decrease of the PLLA concentration in the sheath solution increased the Young's moduli of the fibers, and the best tensile stress was performed by the membranes with 5 wt% PLLA concentration (Fig. 8). The possible reason was that the smaller diameter of fibers with a decrease in the concentration of the sheath solutions caused an increase in mechanical performance, base on the Griffith theory [58]. Similarly, Su et al. [37] also encapsulated TCH into poly (L-Lactide-co-caprolactone) (PLLACL) as the sheath. In this work, a comparison of drug release behavior was made between two different fibrous membranes that were prepared separately by the single-fluid electrospinning and the coaxial process. The results clearly indicated that membranes derived from coaxial process showed a relatively more stable release behavior of the drug TCH without an initial burst release.

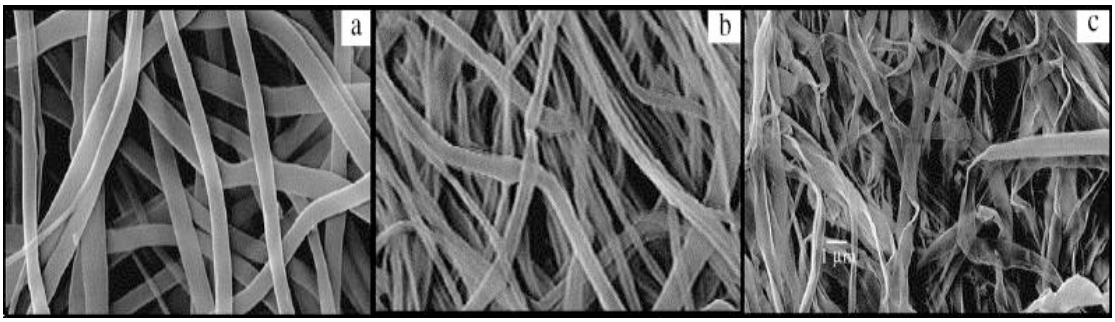

Figure 7 Morphology change of core-sheath structured composite nanofibers prepared by coaxial electrospinning of PCL as the sheath and PEG/lysozyme as the core. The displayed membranes were incubated in 0.05 M, pH 7.4 PBS for (a) 0, (b) 7, and (c) 24 days. The figure displayed gradual collapse of the nanofibers due to the sustained release of the core content. Reprinted from Reference [34].

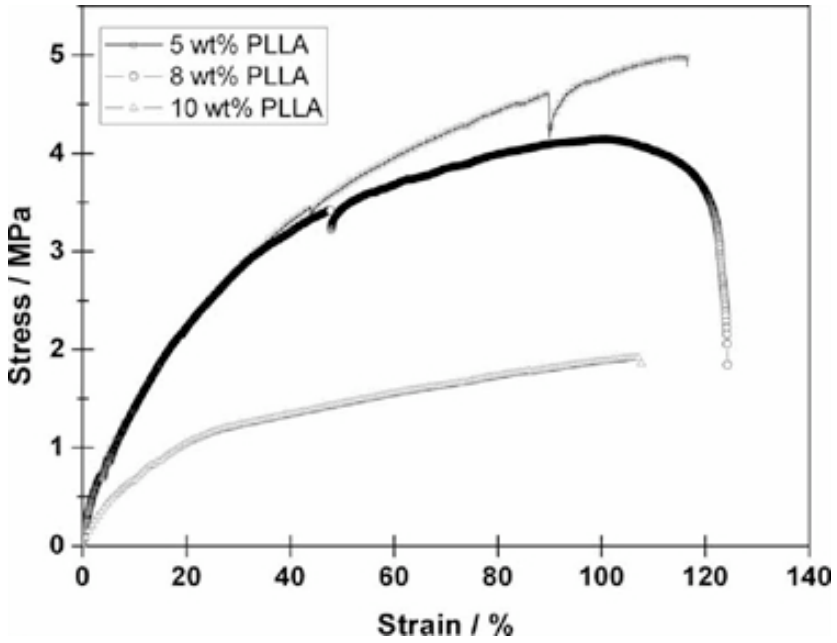

Figure 8 Comparison of tensile stress of the core-sheath fibrous membranes fabricated by using different PLLA concentrations. Reprinted from Reference [55].

Besides improving the drug release profiles, core-sheath fibers can also enhance the physical properties of the fibers compared to single-component fibrous scaffolds. The physical performance has been studied by Sun et al. [37] and Zhao et al. [53]. Sun et al. [37] reported that when compared with electrospun PLA fibrous membranes, PVP-PLA (core-sheath) fibers showed better flexibility and deformability; moreover, the core-sheath fibers displayed greater water absorption ability due to the increase in the aspect ratio and specific surface area of the membranes. They suggested that such fibers could be used as drug delivery systems and tissue engineering scaffolds for loading bioactive agents. Zhao et al. [53] demonstrated that PCL-gelatin (core-sheath) fibrous membranes could combine the advantages of both PCL and gelatin. For future applications of core-sheath fibrous scaffolds in tissue engineering, glutaraldehyde was selected as a model cross-linker for stabilizing the outer water-soluble gelatin layer. The presence of hydrophobic PCL could significantly enhance the mechanic strength of the membranes as well as increase the stress at break of the

hydrated and cross-linked membranes. In addition, the outer gelatin layer could be used to stimulate cell adhesion, proliferation and differentiation of various bioactive agents, such as DNA and growth factors. The interaction between cells and core-sheath fibrous scaffolds at the molecular biology level are displayed in Fig. 9. The results indicated that compared to the electrospun PCL membranes, the core-sheath scaffolds showed a better cell proliferation rate.

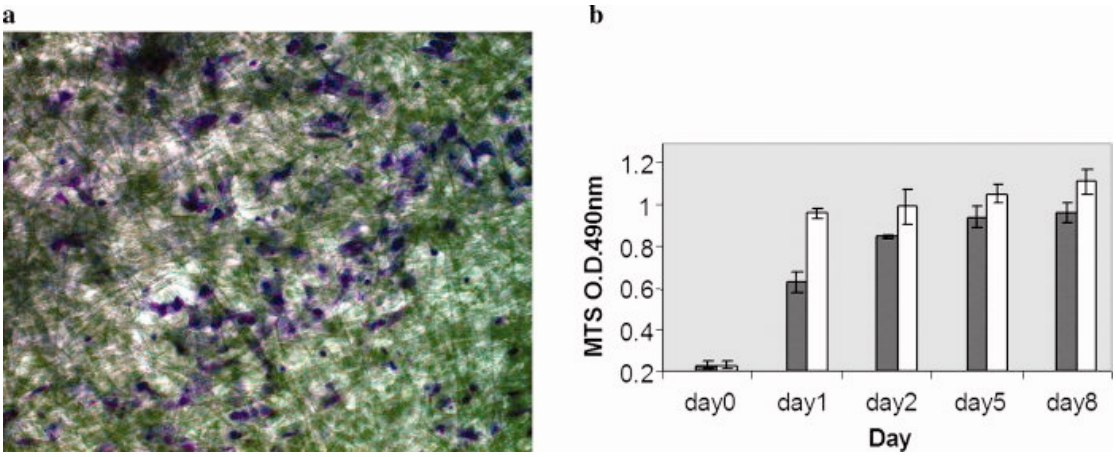

Figure 9 (a) Representative cell-laden, core-shell fibrous scaffolds stained with Crystal violet (after 2 days of incubation). (b) Proliferation of mouse dermal fibroblasts seeded on the fibrous scaffolds composed of PCL (left column) and gelatin-coated PCL (right column). The core-shell fibrous scaffolds were prepared at an inner dope feed rate of 5 mL/h. Glutaraldehyde/gelatin weight ratio was 1.5. Reprinted from Reference [53].

3.2 Hollow structured nanofibers

Hollow structured nanotubes have attracted great attention due to their various applications [46, 59-61], such as catalysis, fluidics, purification, separation, gas storage, energy conversion, sensing, and environmental protection. Compared to other methods, such as self-assembly and template synthesis, coaxial electrospinning is a simple technique for generating nanotubes (Fig. 10).

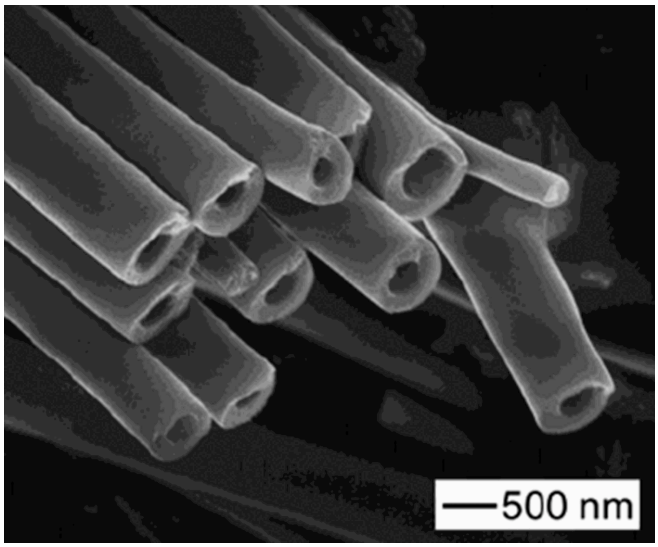

Figure 10 Hollow structured nanofibers prepared by coaxial electrospinning. Reprinted from Reference [46].

Although the concept of electrospinning core-sheath fibers or hollow fibers seems to be straightforward, material requirements for coaxial electrospinning are complex. Three basic material requirements, as concluded by Li and co-works [46, 47, 50, 62], are: (1) both the core and sheath solution should be sufficiently viscous; (2) immiscibility of core and sheath solutions, including solvents, was the key for the formation of uniform hollow structured fibers; (3) The sheath materials must have very good mechanical strength for preparing robust nanotubes.

Some researchers [16, 21, 30, 48] might not agree with the second material requirement because they have successfully electrospun two miscible solutions into core-sheath structured fibers. Li et al. [46] explained that so far they have not shown any hollow structured fibers that were directly prepared by removing the core material of their electrospun fibers. There were two possible drawbacks regarding their core-sheath fibers: the organic polymer nanotubes were not strong enough to maintain the tubular morphology

during the removal of the core material; and the two partially mixed layers of core-sheath fibers were difficult to obtain well-defined hollow structured fibers.

In a study by Li et al. [46], they showed a typical procedure for preparation of nanotubes by coaxial electrospinning (Fig. 11). They reported that the heavy mineral oil as the core and PVP/$Ti(OiPr)_4$, dissolved in ethanol, as the sheath were electrospun to form continuous nanofibers with a core-sheath structure (middle panel). To show the core-sheath structure clearly, the resulted fibers had been extracted with octane to remove the oil core, followed by calcination in air at 500 ^{o}C. The resultant walls of these tubes were titania-nanotubes.

Li et al. [46] reported that the flow-rate for the mineral oil phase (core) played an important role in determining the structure and diameter of the fiber. The inner diameter and wall thickness of the hollow fibers showed in Fig. 11 were 200 and 50 nm, respectively. The authors also tried to electrospin mineral oil and pure PVP into a core-sheath structure, but failed. Based on this result, the authors hypothesized that the hydrolysis and condensation of $Ti(OiPr)_4$ enhanced the viscosity of the PVP solution, and thus allowed the PVP sheath to transmit the viscous stress to the interface between the core and the sheath more effectively during the electrospinning process, resulting in a more stable Taylor cone and jet stream. Moreover, the addition of $Ti(OiPr)_4$ also improved the mechanical strength of the resultant fibers.

In a study by Bazilevsky et al. [42], they reported that poly(methylmethacrylate) (PMMA) as the core and PAN as the sheath also could be electrospun into core-sheath structured fibers, and heat treatment in a nitrogen atmosphere converted these PMMA-PAN

fibers into turbostratic carbon tubes. Loscertales et al. [63] have successfully prepared hollow structured nanotubes in a similar way.

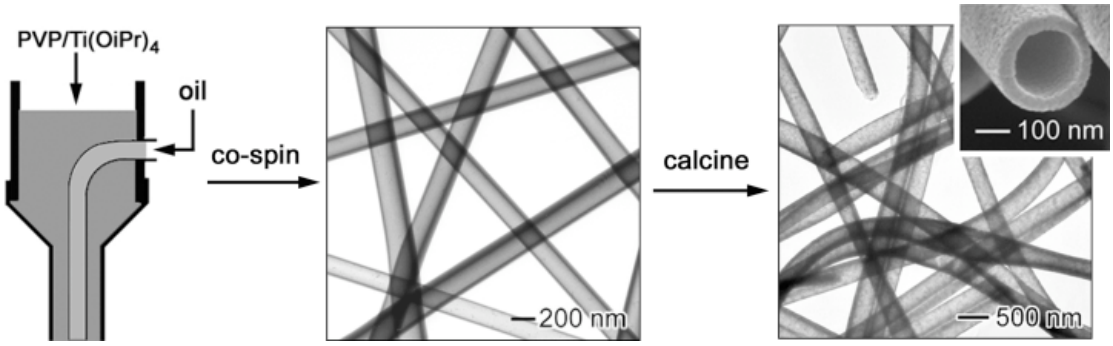

Figure 11 Scheme showing a typical procedure for direct preparation of ceramic nanotubes by coaxial electrospinning. Reprinted from Reference [46].

One of the most recent studies by Srivastava et al. [38] showed that a single cast 2D-hydrodynamic fluid focusing elastomeric device (Fig. 12) could also be used to electrospin two immiscible solution into core-sheath and/or hollow structured nanofibers. In this study, the authors reported that the hollow composite nanofibers of PVP & TiO_2 were synthesized from PVP & $Ti(OiPr)_4$/heavy mineral oil nanofibers by extracting the oil with octane. $Ti(OiPr)_4$ in the sheath layer was rapidly hydrolyzed to TiO_2 in the moist air. Compared to the coaxial electrospinning, this device permitted electrospinning over a wide range of sheath flow-rate ratios for a fixed core flow-rate. The sheath/core volumetric flow ratio could be up to ~40:1 in a proper experimental condition. However, the flow ratio for coaxial electrospinning could only be carried out over a small range of feeding ratio.

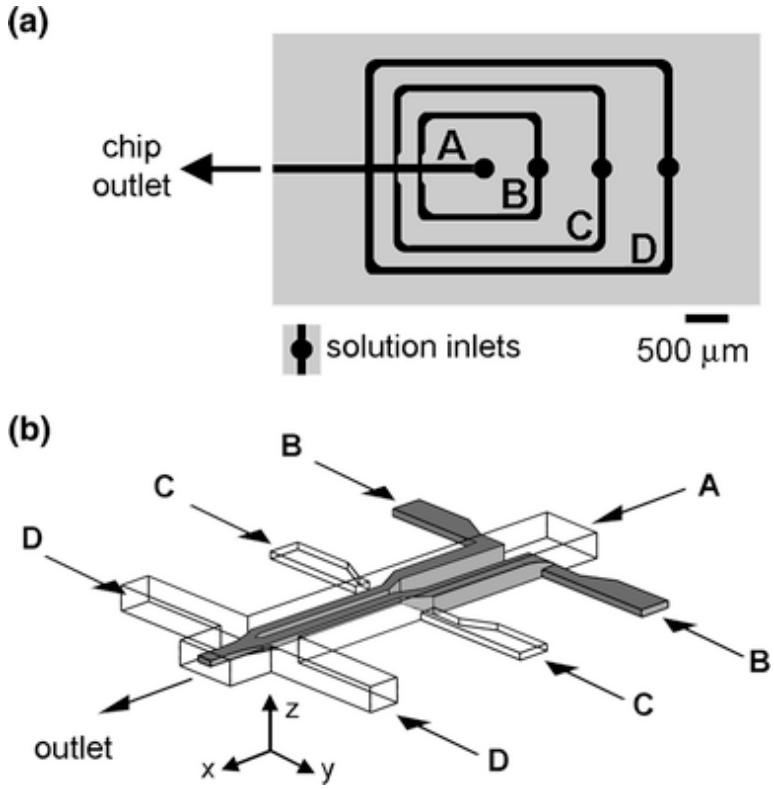

Figure 12 (a) Top–down schematic representation of the micro-channel layout in the PDMS 2D flow-focusing device. The sheath fluid was introduced through inlets A, C and D, while the core fluid was introduced through inlet B. (b) Illustration of the 2D flow-focusing process in the micro-fluidic device. Core fluid enters the central micro-channel at the A–B junction, was initially focused in the vertical direction at the A–C junction, and subsequently focused laterally into a single stream at the A–D junction prior to exiting the device. Reprinted from Reference [38].

3.3. Core-sheath nanofibers for other potential applications

Besides the controlled release system and hollow structured nanotubes, the core-sheath nanofibers for other potential applications have been reported, such as Han et al. [48], Song et al. [64] and Yu et al. [49]. Han et al. [48] demonstrated that a super-hydrophobic and oleophobic material with low surface energy could be easily produced by coaxially electrospinning PCL (core) and Teflon AF (sheath) into core-sheath structured fibers. As expected, the fibers showed good porosity, roughness and stiffness. More importantly, compared to a PCL-only fiber membrane, the PCL/Teflon AF fibrous membrane showed

excellent water bouncing behavior at the water-falling speed of 1.44 m/s with 10 μL volumes, as shown in Fig. 13. This result clearly indicated that the core-sheath fibrous membrane surface structure, including macro-roughness (spacing between fibers) and micro-roughness (striation of individual fibers), very effectively preserved the water-shedding properties of energetic water streams. The authors suggested that this super-hydrophobic material could be very useful in many industries, such as micro-fluidics, textiles, construction and automobiles.

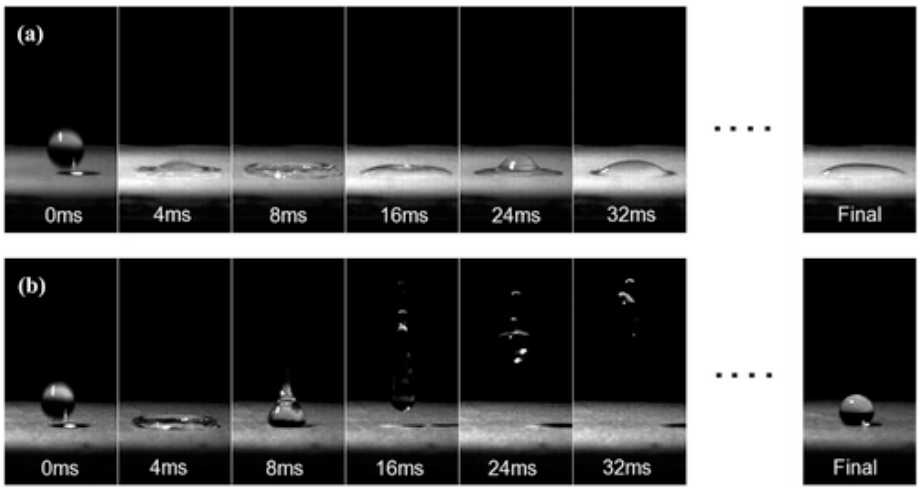

Figure 13 Time sequence of water droplet impact on (a) PCL-only fibrous membranes and (b) core-sheath fibrous membranes. Reprinted from Reference [48].

In a study by Song et al. [64], they presented a simple approach for encapsulating self-assembled iron-platinum (FePt) magnetic nanoparticles in PCL nanofibers by coaxial electrospinning. Such nanoparticle-containg fibers exhibited magnetic behavior, as demonstrated by a typical hysteresis loop obtained using an alternating gradient magnetometer. The fibers could offer a good potential in magnetic and electronic applications, such as smart materials. Additionally, Li et al. [47] have encapsulated conductive materials (poly[2-methoxy-5-(2-ethylhexyloxy)-1,4-phenylenevinylene] (MEH-PVP) or MEH-PVP/PHT) that could not be electrospun into fibers using other encapsulation methods due to limited solubility, into the PVP polymer layer. MEH-PVP has been widely

studied for its excellent luminescent properties and device applications in light-emitting diodes and solar cells. Compared with spin-cast films, these core-sheath fibers displayed a more extended conformation and better spatial orientation. The authors suggested that encapsulation of conductive materials into polymer sheath presented an opportunity for use in electronics and semiconductor applications.

Yu et al. [49] have demonstrated the method of making non-spinnable core fibers by coaxial electrospinning. The concept of making core fibers at the nano level (Fig.14) opposite to that of making hollow fibers.

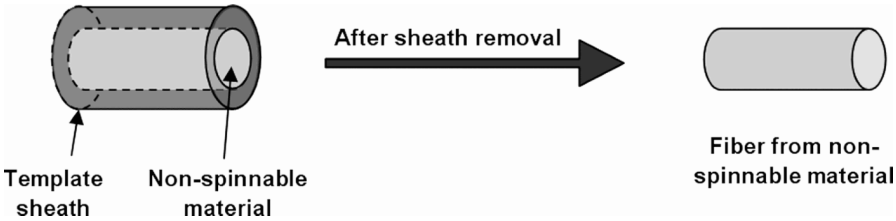

Figure 14 Schematic of fiber formation from non-electrospinnable material. Reprinted from Reference [29].

In this study, the sheath was selectively removed, instead of the core, in order to obtain core fibers. 3 wt% PAN solutions were too dilute to electrospin into fibers using single-fluid electrospinning. However, the authors successfully generated ultrafine fibers from 3 wt% PAN solution by continuously incorporating this dilute solution as the core into polymer solution, PAN-co-PS, that is suitable for electrospinning, using coaxial electrospinning, and then remove the sheath material by dissolving it in chloroform. The resultant PAN fibers had average diameters of 65 nm with a fairly uniform size distribution. Zhao et al. [53] adopted the same approach to prepare core fibers (PCL) by using gelatin as the sheath layer.

4. Research project

Poly(ε-caprolactone) (PCL) is one of the Food and Drug Administration (FDA)-approved biodegradable polymers and has been used in medical and drug delivery devices [65-67], due to its facile accessibility, variable biodegradability, a lack of toxicity, great permeability and good mechanical properties. Herein PCL was selected as a model sheath material. On the other hand, Water-soluble poly(ethylene glycol) (PEG) was selected as the model core polymer. PEG is a biocompatible polymer with excellent fiber-forming property. A mixture of water-soluble bioactive agents can be loading into PEG solution to form the core while PCL works as a protective wall. Moreover, it was reported that PEG could enhance the stability of fragile bioactive macromolecules such as BSA and lysozyme [34, 52].

Electrospun PCL-based polymers or polymer blends have been studied extensively by using different solvents [51, 56, 64], for examples, chloroform, tetrahydrofuran (THF), 2, 2, 2-trifluoroethanol (TFE) and dichloromethane, etc. TFE is one of the suitable solvents for both core PEG and sheath PCL in the coaxial process [51, 56]. In this project, we successfully prepared core-sheath structured fibers by dissolving PEG and PCL in the *same* solvent, TFE. The fiber morphology at different PCL solution concentrations, voltages and flow-rates has been studied. And the surface morphology and physical property of the PEG-PCL core-sheath fibers was characterized by scanning electron microscope (SEM), ^{1}H NMR, thermogravimetric analysis (TGA), water uptake analysis, tensile strength and porosity measurements.

4.1. Experimental section

4.1.1. Materials

PCL was purchased from Sigma-Aldrich, Inc., with a number average molecular weight M_n of 8.0×10^4 Da. Poly (ethylene glycol) methyl ether (mPEG) was also obtained from Sigma-Aldrich, Inc., with a number average molecular weight M_n of 5.0×10^3 Da. The solvent 2, 2, 2-trifluoroethanol (TFE, > 99.0%) was purchase from Sigma-Aldrich, Inc. and directly used as received without further purification.

4.1.2. Preparation of electrospun PCL-only fibers

PCL was dissolved in TFE solvent for 48 hours to produce homogeneous solutions with a concentration range of 10-30 wt%. The spinneret diameter was 0.7 mm. The spinneret tip-to-collector distance was 12 cm. The solutions were then electrospun under high voltages of 10-25 kV and at flow-rates of 10-30 μL/min. The electrospun fibers were collected on a metal drum (diameter: 9 cm) wrapped by an aluminum foil with 400-rmp rotating speed. The electrospun film was dried in a vacuum oven at room temperature over a week.

4.1.3. Preparation of electrospun core-sheath fibers

PEG (10-30 wt%) was dissolved in TFE solvent for 6 hours until they became homogeneous solutions. The coaxial spinneret was composed of inner and outer needles with diameters of 0.5 mm and 1.5 mm, respectively. The spinneret tip-to-collector distance was 12 cm. The PCL solution (20 wt%) as sheath and the PEG solution as core was electrospun onto a rotating drum (diameter: 9 cm; speed: 400 rpm) under a voltage of 15 kV. The flow-rate for

PCL solution was 20 μL/min, and that of PEG solution was in a range of 2-5 μL/min. The other processing conditions were the same as described in 4.1.2.

4.1.4. Water uptake

Three pieces of electropun PCL-only scaffolds and PEG-PCL core-sheath membranes with different core diameters (with PEG content in the core) were cut into a rectangular shape 5 mm x 7 mm with a dry weight (W_b) of about 50 mg. Each specimen was accommodated in a capped vial filled with 10 mL of phosphate buffer (PBS, pH=7.2) and were placed in a constant temperature water bath at 37 ± 0.1 ^{o}C. After 24 hours, three specimens were recovered, wiped with a tissue paper (W_a), and then weighted immediately.

The water uptake percentages of the samples were calculated with the following equation:

$$Water\text{-}Content\% = (W_a - W_b)/W_b \, x \, 100 \qquad (1)$$

with W_b *and* W_a being the mass of membranes before and after immersion in the medium, respectively.

4.1.5. Determination of the porosity of the polymer membranes

The density and the porosity of PCL-only scaffolds and PCL-based hollow fibrous membranes were determined by measuring the mass and dimensions of the membranes. The density (d) of the membrane was calculated as

$$d = m/V \qquad (2)$$

with m and V being the mass and the volume of the membrane, respectively.

The porosity of the membrane, p, was calculated with the following equation:

$$p = (1 - d/d_{PCL}) \times 100 \qquad (3)$$

with d_{PCL} being the density (d_{PCL} = 1.15 g/cm^3) of the PCL polymer.

4.1.6. Characterization instruments

Viscosity measurements: Viscosity measurements were performed using a stress-controlled viscometer (Model Physical MCR 301) manufactured by Anton-Paar, USA, and equipped with parallel plate geometry (diameter 25 mm). The solutions were prepared as described in 4.1.2 and 4.1.3.

Conductivity meter: The conductivity was measured by using a Conductivity Meter (Con 11 Series), manufactured by Eutech Instruments, Singapore. The solutions were prepared using the methods described in 4.1.2 and 4.1.3.

Scanning electron microscope (SEM): The SEM images were obtained by using an SEM, LEO 1550 equipped with Schottky field emission gun (10 kV) and Robinson backscatter detector. The cross-sectional samples were prepared by fracturing the water-wetted fibers in liquid nitrogen. Before SEM observation, the samples were coated with gold for 60s to minimize the charging effect. All fiber diameters were measured and statistically analyzed by using the Leica Microscopy Imaging processing software.

^{1}H NMR: ^{1}H NMR spectra of the PCL-based fibers with/out PEG in the core were recorded on an Oxford NMR AS400 by using $CDCl_3$ as solvent.

Thermogravimetric Analyzer (TGA): TGA analysis was carried out on a Thermogravimetric Analyzer made by PerkinElmer Life and Analytical Sciences, USA. The

temperature rising rate was 10 ºC/min. A small amount of sample (~10 mg) was used for each analysis.

Tensile measurements: Tensile strength was detected on an Instron 4442 instrument. Each specimen was 10 mm x 6 mm, with a thickness of about 0.05 mm. The stretching speed was set at 10 mm/min.

4.2. Results and Discussion

4.2.1. Fabrication of electrospun PCL-only fibers

A series of PCL solutions with concentrations in the range of 10-30 wt% were first electrospun in the single-spinneret mode. These experiments were performed to investigate the effects of materials and processing parameters (PCL solution concentration/viscosity, applied voltage and flow-rate) on the morphology and size of electropun PCL-only fibers in order to find out the best electrospinning conditions of PCL solution for future use with respect to the coaxial electrospinning process

PCL concentration in TFE (%)	10	13	16	18	20	22	25	30
Viscosity (x10^3 cP)	0.1	0.23	0.46	0.73	1.2	1.6	3.0	7.3

Table 4 Properties of PCL solution

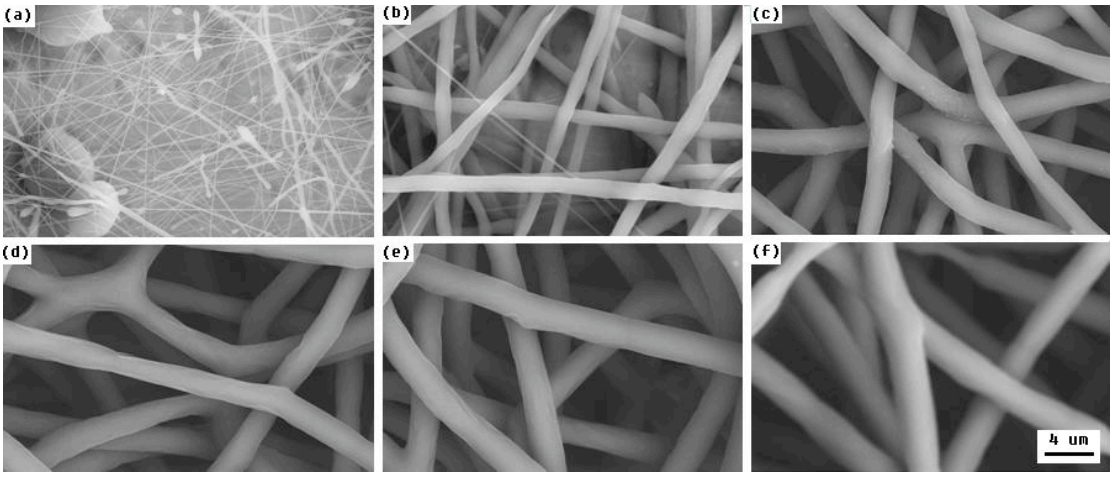

Figure 15 SEM micrographs of electrospun PCL fibers obtained from PCL solutions in TFE with different concentrations under 15 kV voltage and 20 μL/min flow-rate, and all other conditions were described in section 4.1.2. (a) 10 wt% (beads); (b) 13 wt% [diameter (d): 1.6 ± 0.23 μm]; (c) 16 wt% [d: 2.6 ± 0.29 μm]; (d) 18 wt% [d: 2.8 ± 0.29 μm]; (e) 20 wt% [d: 3.1 ± 0.18 μm]; (f) 22 wt% [d: 3.5 ± 0.44 μm]. The average diameter and corresponding uncertainty of the fibers were obtained by measuring 20-30 fibers in SEM images.

The viscosity of PCL solutions increased dramatically with increasing concentration, ranging from 100 cP (10 wt%) to 7300 cP (30 wt%), as listed in Table 4. The fiber morphologies and sizes fabricated from different PCL concentrations (10-22 wt%) were displayed in Fig. 15. When the PCL solution concentration exceeded 20 wt%, it was too viscous for the polymer solution to be electrospun using the current setup. For the 30 wt% solution that had a viscosity of 7300 cP, the solution droplet dried out at the spinneret tip before the jet stream could be properly initiated, and thereby preventing successful electrospinning. Fig 15a shows heavily beaded fibers, indicating that 10 wt% PCL solution was too dilute to produce continuous smooth fibers, and the fibers were still wet when reaching the collector due to insufficient time for solvent evaporation under the current electrospinning conditions. With increasing the PCL concentration from 13 to 22 wt%, the fiber size was increased uniformly. For example, a 20 wt% PCL solution could generate fine fibers with diameters of 3.1 ± 0.2 μm.

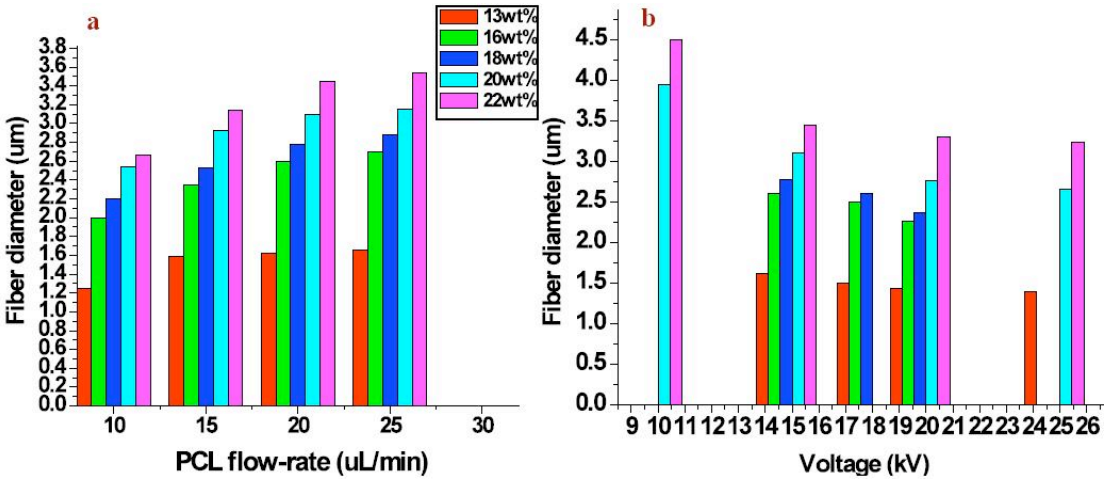

Figure 16 Changes in fiber diameter with different PCL solution concentrations (a & b), flow-rates (a), and voltages (b) at conditions described in section 4.1.2. The average diameter and corresponding uncertainty of the fibers were obtained by measuring 40-50 fibers in SEM images.

Fig. 16a shows the fiber diameters variation at different PCL flow-rates. Obviously, the fiber size for all PCL concentrations was increased by increasing PCL flow-rate. For 20 wt% PCL solution, upon increasing the flow-rate from 10 to 25 µL/min, the fiber diameter increased gradually from 2.5 ± 0.2 to 3.4 ± 0.24 µm. When the flow-rate of all PCL solutions reached 30 µL/min, the electrospun fibers were formed with some beads and droplets on the collection target since the large amount of PCL solution in the spinneret did not have a chance to dry prior to reaching the collector.

Fig. 16b shows a slight decrease in fiber size upon increasing the applied voltage. The thinnest fibers (1.4 ± 0.22 µm) were produced from 13 wt% PCL solution (the lowest concentration) under a voltage of 25 kV (the largest voltage) and a spinneret to collector distance of 12 cm. By contrast, the thickest fibers (4.5 ± 0.26 µm) were generated from 22 wt% PCL solution (the highest concentration) under a voltage of 10 kV (the lowest voltage)

with the same 12 cm distance. As the voltage was increased to 30 kV, the beaded fibers and/or droplets were observed at all PCL concentrations (13-22 wt%).

The above results indicate that the best fibrous membrane (fiber morphology, size, and uniformity) was fabricated from 20 wt% PCL solution with a flow-rate of 20 μL/min under a voltage of 15 kV and spinneret to collector distance of 12 cm (Fig. 15e and Fig 16). Therefore, the 20 wt% PCL solution was chosen as the sheath solution for the study of coaxial electrospinning in the current system.

4.2.2. Fabrication of electrospun core-sheath structured fibers

Solutions in TFE	20 wt% PCL	10 wt% PEG	20 wt% PEG	30 wt% PEG
Conductivity (uS/cm)	0.58	7.01	8.92	9.12

Table 5 Conductivity of PCL and PEG solution for coaxial electrospinning

Solution conductivity is one of the important parameters for the electrospinning process, especially to the coaxial mode. Higher core conductivity usually will cause a discontinuous core material in the fibers because core has significant higher charge density than sheath, which is being pulled by the applied voltage at a faster rate than the feed line can supply. Ideally, sheath solution should have higher or similar conductivity with core solution. Table 3 shows that both PEG (core: ~8.3 uS/cm) and PCL (sheath: 0.58 uS/cm) solutions had very low conductivity values, and therefore they could be used directly for the coaxial process without solution conductivity modification.

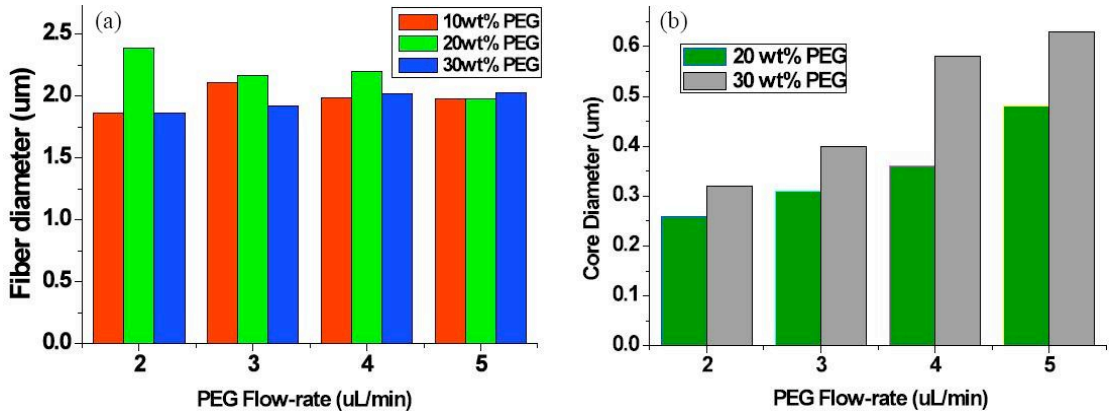

Figure 17 Average overall fiber diameter (a) and core diameter (b) as a function of PEG flow-rates. The core diameters were measured by cross-sectional SEM images showed in Fig. 19. The average diameter and corresponding uncertainty of the fibers were obtained by measuring 30-40 fibers in SEM images. The preparation conditions were described in section 4.1.3.

Fig. 17 shows the overall fiber diameter and core diameter variations of the core-sheath fibers at different PEG concentrations and flow-rates. The overall fiber diameters varied only over a small size range by changing both the PEG concentration and the flow-rate in the inner spinneret (Fig. 17a). By contrast, the core diameters were significantly enhanced by increasing either the PEG concentration or the corresponding flow-rate in the inner spinneret, as shown in Fig.17b. For example, by increasing the flow-rate of the PEG solution (20 wt%) from 2 to 5 μL/min enlarged the core diameters from 0.25 ± 0.06 to 0.46 ± 0.08 μm. In addition, PEG solution with higher concentrations (30 wt%) produced larger core diameters if other conditions were kept the same (Fig. 17b). When the flow-rate of the PEG solution (30 wt%) was increased from 2 to 5 μL/min, the core diameter was increased from 0.32 ± 0.07 to 0.61 ± 0.06 μm. The results indicate that either higher PEG concentration or corresponding flow-rate increased the core diameter, as being determined by the higher PEG content in the core-sheath fibers. In conclusion, both the inner concentration and flow-rate played an important role in the formation of core diameter but had little effect on the overall fiber diameter.

In addition, both core and sheath solution should be delivered at an appropriate flow-rate ratio to keep the core-sheath jet stream continuous. In this PEG as the core and PCL as the sheath system, the 100% loading efficiency was achieved when outer/inner flow-rate ratio was in a range of 10:1 to 4:1 (20 wt% PCL sheath solution: 20 μL/min; 30 wt% PEG core solution: 2 to 5 μL/min). In other words, 2-5 μL/min was the best flow-rate range for the inner solution in this series of experiments, and the coaxial electrospinning could not work properly with feeding ratio out of this range.

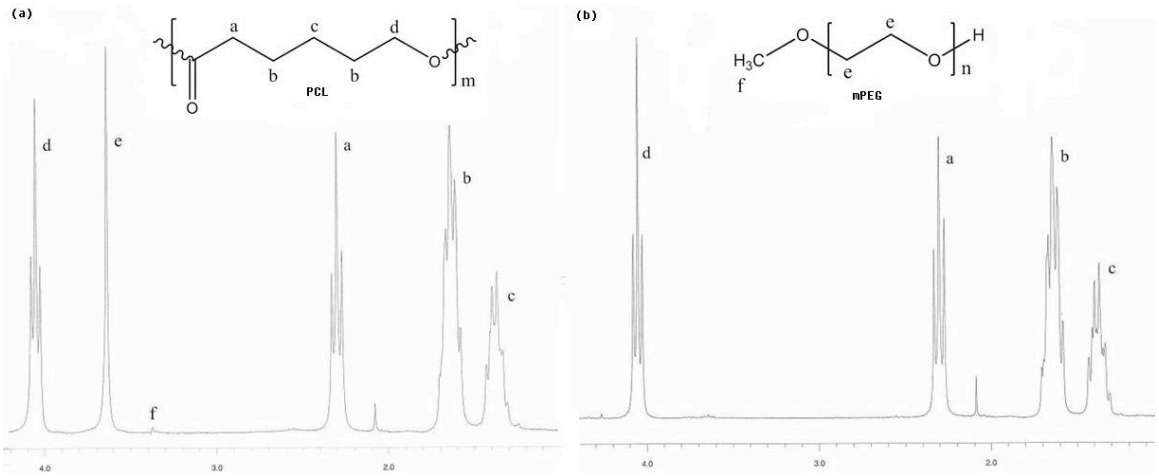

Figure 18 ^{1}H NMR spectra of PEG-PCL core-sheath fibrous membranes (a) before and (b) after removing PEG. Water-soluble PEG core was selectively removed by water extraction.

^{1}H NMR spectra were used to determine if PEG was completely extracted after immersing the core-sheath membranes in water for a week. Fig. 18 shows the PCL and PEG characteristic peaks of core-sheath fibrous membranes before and after removing PEG. It is noted that the PCL characteristic peaks at around 1.35, 1.64, 2.30 and 4.05 ppm were shown in both spectra. By contrast, the PEG characteristic peaks at 3.37 and 3.63 ppm were only displayed in the spectrum of the membranes before removing PEG (Fig. 18a), and

disappeared after removing PEG (Fig. 18b), indicating successful removal of PEG by water extraction, although the absence of PEG characteristic peaks could not ascertain its complete removal.

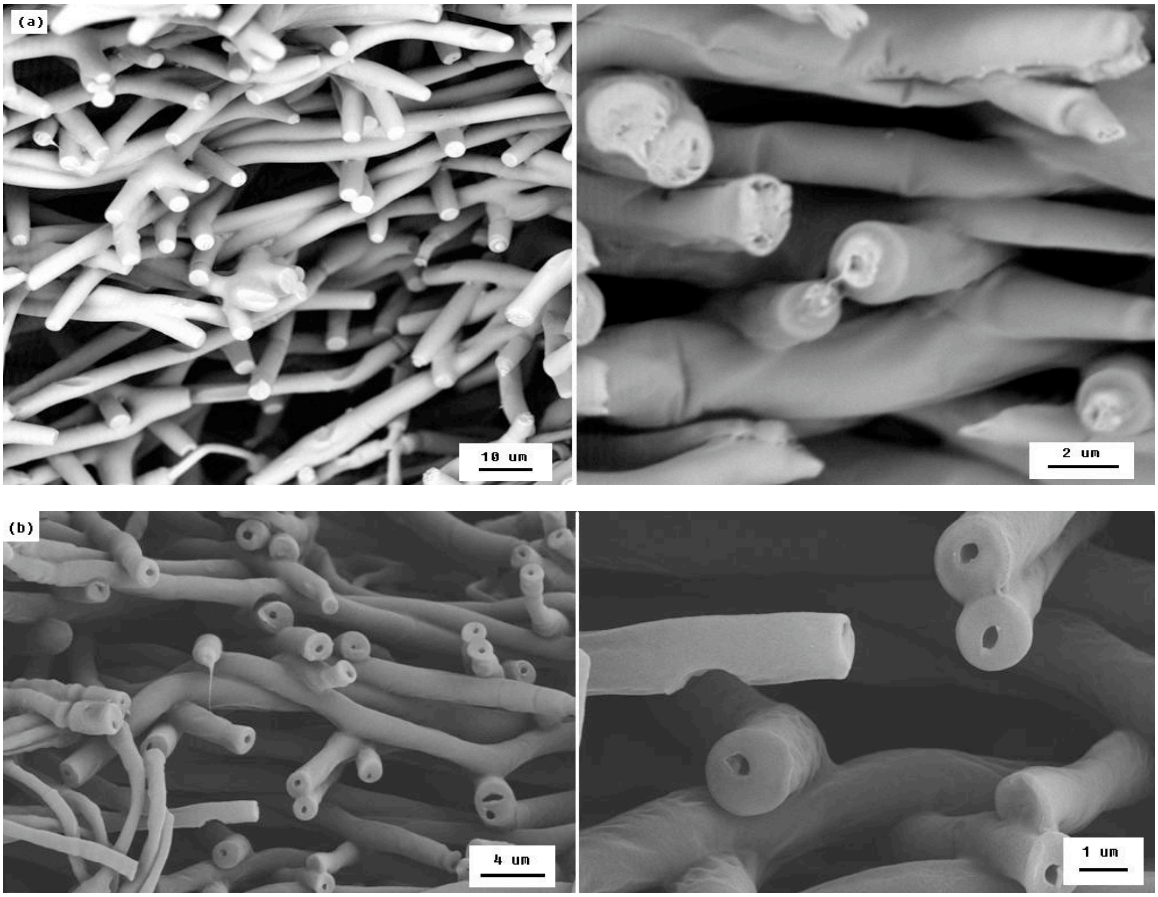

Figure 19 Cross-sectional SEM micrographs of core-sheath fibers (a) before and (b) after removing PEG. The PCL-based hollow structured fibers (b) were obtained from selective removal of the water-soluble PEG core by water extraction. These fibers with holes in the center were used to calculate the core diameter and the wall thickness. The average core diameter and wall thickness of the fibers were obtained by measuring 10-20 fibers in SEM images. In the preparation of all these samples, the concentrations of PEG and PCL solution dissolved in TFE were 30 wt% and 20 wt%, and the flow-rates of both solutions were 3 μL/min and 20 μL/min, respectively. The voltage of electrospinning was 15 kV. Other conditions were the same as described in section 4.1.3.

To further confirm the encapsulation of PEG in PCL fibers, a cross-sectional SEM was performed to show the core-sheath structure of the fibers before and after removing the core content (Fig. 19), with PEG as the core and PCL as the sheath, while both solutions

were dissolved in the same TFE solvent and were coaxially electrospun to form continuous core-sheath structured fibers. Fig. 19a shows some fibers with solid core structures. The color contrast between the polymer in the center and that in the outer layer indicates that they are composed of two different materials, presumably PEG as the core and PCL as the sheath. Selective removal of the water-soluble PEG core by water extraction gave tubular fibers with a PCL-based wall. The images in Fig. 19b clearly show the formation of hollow structures, uniform in size, with an inner diameter and wall thickness of 0.4 ± 0.11 μm and 0.63 ± 0.14 μm. By controlling the inner spinneret concentration and the corresponding flow-rate, the core diameters of the nanotubes could be adjusted (Fig. 17b). The SEM image confirmed that the PEG contents were encapsulated as a relatively uniform thread in each fiber during the coaxial electrospinning process; otherwise the images could not show those holes in the center of the fibers.

4.2.3. TGA analysis

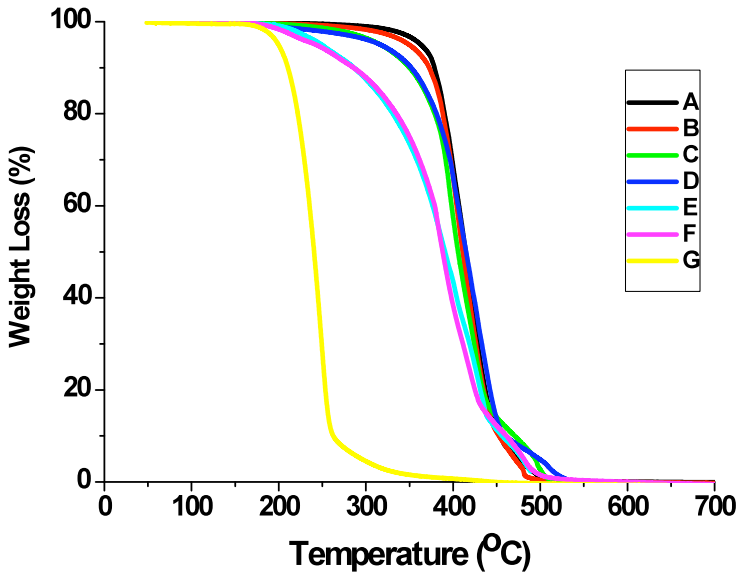

Figure 20 TGA profiles of PCL fibers, PEG-PCL fibers and pure PEG: A) PCL-only fibrous membrane; B) PCL-based hollow structured membrane after the removal of PEG; C-F) PEG-PCL core-sheath fibrous membranes with different core diameters of 0.32, 0.40, 0.58 and 0.61 μm, respectively; G) pure PEG sample. Other conditions: PCL solution: 20 wt% with 20 μL/min flow-rate, PEG solution: 30 wt% with 2-5 μL/min, Voltage: 15 kV. The membrane preparation was the same as described in section 4.1.3.

Sample	Onset (ºC)	Residue (%)	Final (ºC)	Residue (%)
A	377	99	477	0.032
B	379	98	485	0.061
C	297	97	481	0.072
D	266	98	474	2.4
E	219	99	478	5.4
F	204	98	445	5.8
G	191	98	311	1.2

Table 6 Thermogravimetric Onset, Final Temperature, and Residue for all samples. The sample names (A-G) were the same as listed in Fig. 20.

All samples in Fig. 20 showed a one-step weight loss profile, but they had different decomposition rates. A sharp drop on the weight for all samples was likely to be the oxidation combustion of the PCL/PEG main chain. Table 6 shows the thermogravimetric onset, final temperature, and residue of all samples. The pure PEG (G) showed a fast decomposition rate, and it started decomposing at 191 ºC and finished at 311 ºC.

As shown in Table 6, the electrospun PCL-only fibrous membrane (A) started degrading at about 377 ºC and was completely decomposed at 477 ºC. The PCL-based hollow fibrous membrane (B) that was made from the core-sheath membrane (C) by selective removal of PEG content, showed similar onset and final temperatures with the PCL-only membrane (A), about 379 ºC and 485 ºC, respectively. By contrast, the core-sheath membrane with PEG (C) showed an earlier onset temperature of 297 ºC. The results indicate that the PEG content in membrane (B) was successfully removed, and incorporation of PEG in the membrane (C) reduced the thermal stability of overall fibers.

The core-sheath fibrous membranes with different amount of PEG contents started degrading at 297 ºC (flow-rate: 2 μL/min; core diameter: 0.32 μm), 266 ºC (3 μL/min; 0.40 μm), 219 ºC (4 μL/min; 0.58 μm) and 204 ºC (5 μL/min; 0.61 μm), much lower than the PCL-only membranes at 377 ºC (A), as shown in Table 6. Higher PEG flow-rate increased the core diameter, resulted in higher PEG content in the core-sheath fibers, therefore influenced the onset temperature of the decomposition. However, the final temperatures of the degradation were not affected by the incorporation of PEG in the PCL-based fibers, because the PCL could last up to 477 ºC, much higher than the 311 ºC ending temperature of PEG.

In summary, the PCL membranes had higher thermal stability than the core-sheath fibrous membranes containing PEG. The thermal decomposition properties of the core-sheath membranes were significantly influenced by the amount of PEG in the fibers. An increase of PEG content in the fibers decreased the onset temperature, but had little effect on the final decomposition temperature.

4.2.4. Tensile strength

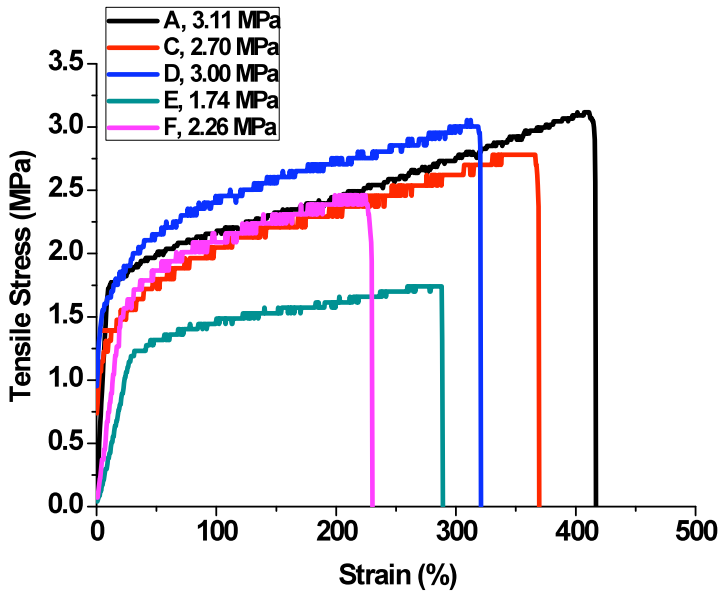

Figure 21 Tensile curves of (A) PCL fibrous membrane, and (C-F) PEG-PCL core-sheath fibrous membranes with different PEG core diameters of 0.32, 0.40, 0.58 and 0.61 μm. The membrane preparation was the same as described in section 4.1.3.

PCL is known for its good mechanical strength. The variation of tensile stress and elongation at break of PCL-based membranes with or without PEG is presented in Fig. 21 and 22.

As shown in Fig. 21, all membranes initially indicated a linear stress increase; however, the onset of nonlinearity was seen at around 10% strain. All membranes were largely stretched with increasing strain. The sudden stress drop was seen with visible membrane fracture. The pure PCL membranes had a tensile strength value of 3.11 MPa, which was decreased to 1.74 MPa with the incorporation of the PEG core. Compared to PCL, the low molecular weight PEG had much lower mechanical strength, causing a decrease in the overall strength of the PEG-containing fibers.

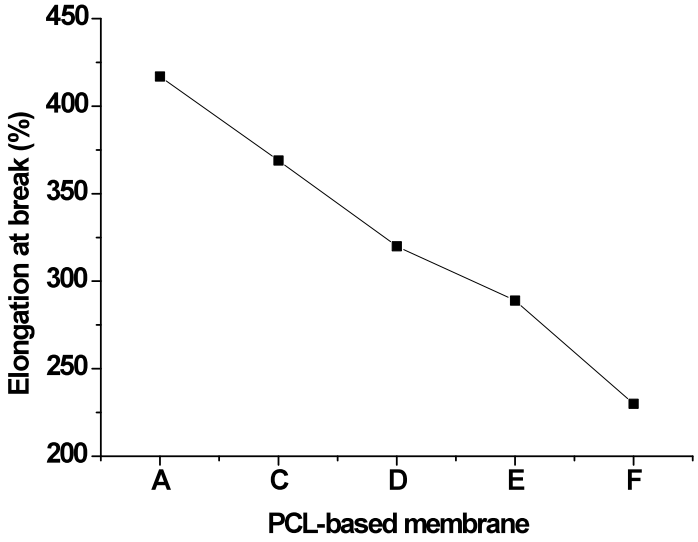

Figure 22 Variations of elongation at break of PCL-based membranes. A) PCL-only fibrous membrane, and C-F) core-sheath fibrous membranes with different PEG core diameters of 0.32, 0.40, 0.58 and 0.61 μm.

Fig. 22 shows the variation of elongation at break of all studied membranes. There was a decrease from the value of 417% for pure PCL membranes (A) to the values of 369%, 320%, 289% and 230% for the core-sheath fibrous membranes with increasing PEG content (C-F). This was because the thickness of the PCL sheath went down by increasing the core diameter, resulting in a weak elongation at break. In summary, the stiffness and the elasticity of the PCL-based fibrous membranes went down with increasing incorporation of PEG content, as to be expected.

4.2.5. Water uptake

Pure PCL membrane was not good at absorbing water due to its hydrophobic property, and it only absorbed 67 ± 7% of water after 24 hours in phosphate buffer. By contrast, the water absorption ability of the core-sheath fibrous membranes increased dramatically by introducing PEG in the core. For examples, the average water uptake values of the PEG-PCL

core-sheath membranes with PEG content in the cores (Core diameter: 0.32-0.61 μm) were 195 ± 11%, 183 ± 8%, 215 ± 23% and 129 ± 31%, respectively. The average water uptake value and corresponding uncertainty of the fibers were achieved by measuring three samples. The result indicated that the water absorption of the core-sheath fibrous membranes was more than that of the pure PCL membranes. A possible reason was that the presence of core-sheath structure in the fibrous membranes increased the aspect ratio and specific surface area for water attachment via diffusion. Furthermore, the incorporation of hydrophilic PEG enhanced the hydrophilicity of the PCL-based membrane, and therefore the membranes became more water compatible. In other words, the PEG in the fibers could make the hydrophobic PCL membranes more water-permeable, thereby providing better biocompatibility with human body.

The water uptake results indicate that not all PEG in fibers were dissolved in 24 hours. The core material was effectively controlled from quickly being released by the PCL shell, and therefore such core-sheath fibrous scaffolds may have potential applications in drug delivery systems and tissue engineering scaffolds for loading bioactive agents.

4.2.6. Porosity

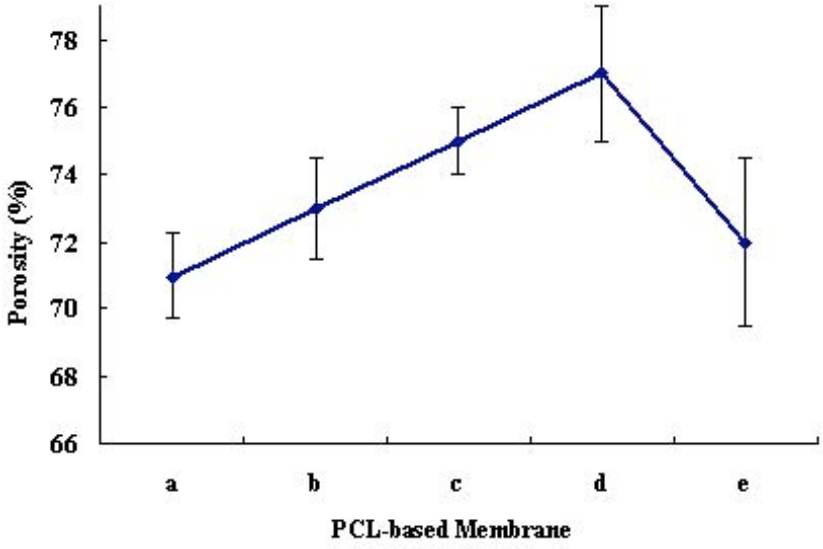

Figure 23 Porosity of electrospun PCL and PCL-based hollow fibrous membranes. a) Electrospun PCL fibrous membrane; and b-e) electropsun PCL-based hollow fibrous membranes (after the removal of PEG content) with different core diameters: (b) 0.32 μm, (c) 0.40 μm, (d) 0.58 μm and (e) 0.61 μm. The average porosity and corresponding uncertainty of the fibers were determined by measuring three pieces of samples. The membrane preparation was the same as described in section 4.1.3.

Fig. 23 shows the porosity of electrospun PCL membrane (a) and PCL-based hollow fibrous membranes (b-e, after the removal of PEG content) with different core diameters. The porosity of the pure PCL membrane (a) was reached 71 ± 1.3%. In contrast with the PCL-only membrane, the PCL-based hollow fibrous membranes (b-e) showed higher porosity values, 73 ± 1.5%, 75 ± 1%, 77 ± 2% and 72 ± 2.5%. This result indicates that in the presence of the hollow structured fibers, the mass of the PCL-based membranes was decreased, but the volume remained similar, resulting in decreased scaffold density and increased porosity values.

Obviously, the porosity values of the PCL-based hollow fibrous membranes (b-d) went slightly higher by increasing the core diameters, except for the membrane with the

largest core diameter (e: 72 ± 2.5%). However, the membrane with the largest core diameter was expected to have the highest porosity value. A possible reason was that the PCL shell was not strong enough to maintain the tubular morphology when the core diameter reached 0.61 μm, with possible thinner sheath, and caused the hollow structured fibers to partially collapse. Therefore, the membrane (e) showed a relatively lower porosity value compared to other hollow fibrous membranes (b-d).

5. Conclusion

We have successfully encapsulated PEG into PCL-based fibers via a coaxial electrospinning process. Moreover, selective removal of PEG contents generated hollow structured fibers with uniform, circular cross-sections, although the complete removal of PEG cannot be proven by the NMR data alone. Both the PEG concentration and the corresponding flow rate played an important role in the formation of the core diameter but showed little effect on the overall fiber diameter. The thermal decomposition properties of the core-sheath fibrous membranes were significantly affected by the incorporation of the PEG content, as PEG was thermally less stable and thereby changing the overall stability of the core-sheath fiber. Pure PCL fibers had higher heat degradation stability when compared with core-sheath fibers with a PCL sheath. In the presence of a hollow structure in the core, the porosity of the membranes was increased. The tensile strength results indicated that the stiffness and the elasticity of the core-sheath fibrous membranes went down along with the incorporation of PEG. The coaxial technique is not limited to PEG and PCL polymers, but can be extended to other polymer systems by using the procedure described here. Such core-sheath/hollow structured fibers may be a promising candidate for potential applications, such as catalysis, sensing, encapsulation, electrical devices, and drug delivery.

References

1. W.E. Teo and S. Ramakrishna. Nanotechnology, 2006, 17, R89-R106.
2. G.I. Taylor. Proc. R. Soc. Lond. Ser., 1969, A313, 453-475.
3. G.I. Taylor. Proc. R. Soc. Lond. Ser., 1964, A280, 383-397.
4. A.L. Yarin, S. Koombhongse and D.H. Reneker. J. Appl. Phys., 2001, 90, 4836-4846.
5. C.X. Zhang, X.Y. Yuan, L.L. Wu, Y. Han and J. Sheng. Euro. Polym. J., 2005, 41, 423.
6. H. Fong, I. Chun and D.H. Reneker. Polymer, 1999, 40, 4585-4592.
7. W. Zhu, M. Zhu, W. Yang, H. Yu, Y. Chen and Y. Zhang. Polym. Eng. and Sci., 2005, 45, 704-705.
8. M. Hohman, Y.M. Shin, G. Rutledge and M.P. Brenner. Phys. Fluids, 2001, 13, 2221-2236.
9. X. Zong, K. Kim, D. Fang, S. Ran, B.S. Hsiao and B. Chu. Polymer, 2002, 43, 4403-4412.
10. S.A. Theron, E. Zussman and A.L. Yarin. Polymer, 2004, 45, 4403-4412.
11. Q.P. Pham, U. Sharma and A. G. Mikos. Polymer Reviews, 2008, 48, 353-377.
12. E.D. Boland, T.A. Telemeco, D.G. Simpson, G.E. Wnek and G.L. Bowlin, J. Biomed. Mater. Reser., 2004, 71B, 144-152.
13. M. Bognitzki, T. Frese and J.H. Wendorff. Abstracts of Paper for the ACS, 2000, 219, U491.
14. C.M. Hsu and S. Shivkumar. Macromol. Mater. and Engin., 2004, 289, 334-340.
15. L. Buttafoco, N.G. Kolkman, P. Engbers-Buijtenhuijs, A.A. Poota, P.J. Dijkstraa, I. Vermesa, J. Feijena. Biomater., 2006, 27, 724-734.
16. Y.Z. Zhang, H.W. Ouyang, C.T. Lim, S. Ramakrishna and Z.M. Huang. J. Biomed. Mater. Res., 2005, 72B, 156-165.
17. B.M. Min, G. Lee, Y.S. Nam, T.S. Lee and W.H. Park. Biomaterials, 2004, 25, 1289-1297.
18. C. Burger, B.S. Hsiao and B. Chu. Annu. Rev. Mater. Res., 2006, 36, 333-368.

19. K. Fujihara, M. Kotaki and S. Ramakeishna. Biomaterials, 2005, 26, 4139-4147.

20. Q. Cui, X. Dong, J. Wang and M. Li. Journal of Rare Earths, 2008, 26, 664-669.

21. Z.M. Huang, Y.Z. Zhang, M. Kotaki and S. Ramakrishna. Compos. Sci. Technol, 2003, 63, 2223.

22. A. Frenot and I.S. Chronakis. Polymer nanofibers assembled by electrospinning, Curr. Opin. Colloid. In., 2003, 8, 64.

23. J. Zheng, X.Y. Xu, X.S. Chen, Q.Z. Liang, X.C. Bian, L.X. Yang and X.B. Jing. Controlled Release, 2003, 92, 227.

24. L.L. Wu, X.Y. Yuan and J. Sheng. Jour. Membr. Sci., 2005, 250, 167.

25. D.H. Liang, B.S. Hsiao and B. Chu. Adv. Drug Deliv. Re., 2007, 59, 1392-1412.

26. H.L. Schreuder-Gibson, P. Gibson, P. Tsai, P. Gupta and G. Wilkes. International Nonwovens Journal, 2004, 13, 39-45.

27. H. Schreuder-Gibson, P. Gibson, L. Wadsworth, S. Hemphill, J. Vontorcik. Advances in Filtration and Separation Technology, 2002, 15, 525-537.

28. C. Drew, X. Liu, D. Ziegler, X.Y. Wang, F.F. Bruno, J. Whitten and L.A. Samuelson. J. Nano Letter, 2003, 3, 143.

29. A. K. Moghe and B. S. Gupta. Polymer Reviews, 48, 353-377.

30. I.G. Loscertales, A. Barrero, I. Guerrero, R. Cortijo, M. Marquez and A.M. Ganan-Calvo. Science, 2002, 295, 1695-1698.

31. Y. Zhang, Z.M. Huang, X. Xu, C.T. Lim and S. Ramakrishna. Chem. Mater. 2004, 16, 3406-3409.

32. X.J. Han, Z.M. Huang, C.L. He and L. Liu. Polym. Compos., 2006, 27, 381-387.

33. Z.M. Huang, C.L. He, A.Yang, Y.Z. Zhang, X.J. Han, J.L. Yin and Q.S. Wu. J. Biomed. Mater. Res, 2005, 77A, 169-179.

34. H.L. Jiang, Y.Q. Hu, Y. Li, P.C. Zhao, K.J. Zhu and W. Chen. J. Contr. Relea. 2005, 108, 237-243.

35. Z. Ahmad, H. Zhang, U. Farook, M. Edirisinghe, E. Stride and P. Colombo. J. R. Soc. Interface, 2008, 5, 1255-1261.

36. X.Q. Li, Y. Su, R. Chen, C.L. He, H.S. Wang and X.M. Mo. J. Appl. Polym. Sci., 2009, 111, 1564-1570.

37. Y. Su, X.Q. Li, H.S. Wang, C.L. He and X.M. Mo. J. Mater. Sci.: Mater. Med., 2009, 20, 2285-2294.

38. Y. Srivastava, C. Rhodes, M. Marquez and T. Thorsen. Microfluid Nanofluid, 2008, 5, 455-458.

39. Q.P. Pham, U. Sharma and A.G. Mikos. Polymer, 2006, 12, 1197-1211.

40. J.M. Deitel, J. Kleinmeyer, D. Harris and N.C.B. Tan. Polymer, 2001, 42, 261.

41. C.S. Ki, D.H. Baek, K.D. Gang, K.H. Lee, I.C. Um and Y.H. Park. Polymer, 2005, 46, 5094.

42. A. Bazilevsky, A. Yarin and C. Megaridis. Langmuir, 2007, 23, 2311-2314.

43. M. Wei, B. Kang, C. Sung and J. Mead. Macromol. Mater. Eng., 2006, 291, 1307-1314.

44. B. Sun, B. Duan and X.Y. Yuan. J. Appl. Polym. Sci., 2006, 102, 39-45.

45. Y. Zhang, Z. Huang, X. Xu, C. Lim and S. Ramakrishna. Chem. Mater. 2004, 16, 3406-3409.

46. D. Li and Y.N. Xia. Nano Letter, 2004, 4, 933.

47. D. Li, A. Babel, S.A. Jenekhe and Y.N. Xia. Adv. Mater., 2004, 16, 2062-2066.

48. D. Han and A.J. Steckl. Langmuir, 2009, 25, 9454-9462.

49. J.H. Yu, S.V. Fridrikh and G.C. Rutledge. Adv. Mater., 2004, 16, 1562-1566.

50. J. McCann, D. Li and Y.N. Xia. J. Mater. Chem., 2005, 15, 735-738.

51. Y.Z. Zhang, X. Wang, Y. Feng, J. Li, C.T. Lim and S. Ramakrishna. Biomacromolecules, 2006, 7, 1049-1057.

52. H.L. Jiang, Y.Q. Hu, P.C. Zhao, Y. Li and K.J. Zhu. J. Biomed. Mater. Res., 2006, 79B, 50-57.

53. P.C. Zhao, H.L. Jiang, H. Pan, K.J. Zhu and W. Chen. J. Biomed. Mater. Res., 2007, 83A, 372-382.

54. I.C. Liao, S.L. Chen, J.B. Liu and K.W. Leong. J. Contr. Rel., 2009, 139, 48-55.

55. C.L. He, Z.M. Huang, X.J. Han, L. Liu, H.S. Zhang and L.S. Chen. J. Macromole. Sci., 2006, 45, 515-524.

56. I.C. Liao, S.Y. Chew and K.W. Leong. Nanomedicine, 2006, 4, 465-471.

57. E.R. Kenawy, G.L. Bowlin, L. Mansfield, D.G. Simpson, G.L. Bowlin, J. Layman and E.H. Wnek. J. Contr. Relea., 2002, 81, 57.

58. R.F. Gibson. McGraw-Hill: New York, 1994.

59. R.H. Baughman, A.A. Zakhidov and W.A. de Heer. Science, 2002, 297, 787.

60. L. Hueso and N. Mathur. Nature, 2004, 427, 301.

61. C.R. Martin and P. Kohli. Nature Rev. Drug Discov., 2003, 2,29.

62. D. Li, J.T. McCann and Y.N. Xia. J. Am. Soc., 2006, 89, 1861-1869.

63. I.G. Loscertales, A. Barrero, M. Marquez, R. Spretz, R. Velard-Oritiz and G. Larsen. J. Am. Chem. Soc., 2004, 126, 5376-5377.

64. T. Song, Y.Z. Zhang, T.J. Zhou, C.T. Lim, S. Ramakrishna and B. liu. Chem. Phy. Lett., 2005, 415, 317-322.

65. F.K. Ko and M.R. Gandhi. Nanofibers and Nanotechnology in Textiles, 2007, 22-24.

66. S.A. Sell and G.L. Bowlin. J. Mater. Chem., 2008, 18, 260-263.

67. L. Zhang, L. Wang and P. Hu. Key Engineering Materials, 2005, 288-289.